IV. MEDIUM-ENERGY NUCLEAR PHYSICS RESEARCH

OVERVIEW

In order to understand how to incorporate the quark-gluon structure of the nucleon into a fundamental description of nuclear forces, the medium-energy research program in the Argonne Physics Division emphasizes the study of processes in nuclei in which interactions with the constituents of the nucleon describe the basic physics. Examining related physics topics at both the quark and hadronic levels in complementary experiments is most revealing of the low-energy structure of the strong interactions. Because energetic leptons provide an accurate, well-understood probe of these phenomena, primary emphasis is placed on the experiments involving electron and muon scattering.

The electron beams of the Thomas Jefferson National Accelerator Facility (TJNAF) are ideally suited for studies of nuclei at hadronic scales and represent one center of the experimental program. Staff members led in the construction of experimental facilities, serve as spokesmen for three experiments and are actively involved in several others. The group completed construction of the broad-purpose Short Orbit Spectrometer which forms half of the coincidence spectrometer pair that is the base experimental equipment in Hall C. We continue to upgrade the SOS detector package and improve the understanding of the spectrometer optics and acceptance. Argonne led the first experiment to be carried out at TJNAF in FY1996 and has completed six other experiments. In FY1999 measurements were made with a 5.5 GeV electron beam to extend our results on the d(γ,p)n and (e,e'p) reactions to higher scales. An experiment was also completed to measure the ratio of the longitudinal to transverse inelastic electron scattering response in the resonance region. We also measured kaon electroproduction on targets of ^{3}He and ^{4}He to study the reaction mechanism of electroproduction of hypernuclei and to search for bound Σ-hypernuclear states.

The first results from TJNAF build upon previous ANL experiments at Stanford Linear Accelerator Center (SLAC), MIT-Bates and Saclay (ALS). For the first time, forward-backward angle measurements of the (e,e'p) reaction have been used to perform longitudinal-transverse separations of the proton spectral function at high momentum transfers. Exclusive deuteron photo-disintegration experiments have established that this reaction obeys quark-counting-rule scaling arguments at large transverse momenta. The simplest extension of this work, to coherent pion photo-production on the deuteron, did not see evidence of the quark counting rule behavior. Measurements of kaon production on hydrogen, deuterium, ^{3}He and ^{4}He provide important information on the basic strangeness production mechanisms, the poorly known low energy hyperon-nucleon interaction and the electromagnetic form factor of the K^{+}. Pion production measurements on hydrogen, deuterium, ^{3}He and ^{4}He will

determine the charge form factor of the pion and measure the change in the pion field in the nuclear medium. Since the pion contains valence antiquarks, these measurements complement our high energy Drell-Yan measurements of the antiquark distributions in nucleons and nuclei. Results of new measurements of inclusive electron scattering in the resonance region provide evidence for the concept of semi-local duality in relating averaged resonance and deep inelastic scattering yields.

HERMES, a broadly based North American-European collaboration is studying the spin structure of the nucleon using internal polarized targets in the HERA storage ring at DESY. Deep inelastic scattering has been measured with polarized electrons on polarized hydrogen and ^{3}He. Argonne has concentrated on the hadron particle identification of HERMES, a unique capability compared to other spin structure experiments. In 1999, the Argonne-led dual-radiator ring imaging Cerenkov counter (RICH) was brought into operation at the design specifications to provide complete hadron identification in the experiment. This will allow HERMES to make decisive measurements of the flavor dependence of the spin distributions. HERMES is beginning to make measurements of the spin dependence of the glue in the photoproduction of pairs of high transverse momenta pions. The HERMES experiment is also making significant advances in unpolarized deep-inelastic scattering physics with its coincident hadron detection. Argonne scientists have extended the physics program in studies of exclusive vector meson production in polarized-beam-polarized-target measurements and also measurements on nuclear targets. Clear evidence is seen on the nuclear targets for the effect of coherence in the production mechanism. An unexpected strong nuclear dependence of the ratio of longitudinal to transverse deep inelastic scattering cross sections has been observed at low x and Q^2. This will be explored further in a TJNAF experiment in 2000.

Measurements of high mass virtual photon production in high energy proton-induced reactions have determined the flavor dependence of the sea of antiquarks in the nucleon. These measurements give insight into the origin of the nucleon sea. In the same experiment, the nuclear dependence of the Drell-Yan process and the nuclear dependence of the production of heavy quark resonances such as the J/ψ and ϒ have been determined. The Drell-Yan results demonstrate that the energy loss of quarks in the nuclear medium is significantly less than theoretical expectations. The heavy vector meson results provide constraints on the gluon distributions of nucleons and nuclei and a significant baseline for attempts to use heavy vector meson production as a signal of the formation of the quark-gluon plasma in relativistic heavy-ion experiments. A new initiative is underway to continue these measurements with much higher luminosity at the FNAL Main Injector.

The technology of laser atom traps provides a unique environment for the study of nuclear and atomic systems and represents a new thrust for the group. Initially the efforts focus on developing high efficiency and high sensitivity trapping techniques for the isotope analysis of noble gases. The isotope Krypton-81 was detected at natural (10^{-13}) abundance and the technique was demonstrated to be free of contamination from other isotopes and elements. This atom trace analysis (ATTA) technique provides a new approach to such diverse problems as dating old ground water or mapping out the atmospheric concentration of fission products. Work has begun on applying ATTA to the detection of ^{41}Ca. A longer term goal is to make nuclear moment measurements of trapped short-lived atoms and to apply these techniques to a variety of weak interaction problems.

A. SUBNUCLEONIC EFFECTS IN NUCLEI

a.1. The Energy Dependence of Nucleon Propagation in Nuclei as Measured in the (e,e'p) Reaction

(D. F. Geesaman, J. Arrington, K. Bailey, W. J. Cummings, D. DeSchepper, H. E. Jackson, C. Jones, S. Kaufman, T. O'Neill, D. Potterveld, J. Reinhold, J. P. Schiffer, B. Zeidman, P. Bosted,* A. Lung,† D. Abbott,‡ R. Carlini,‡ J. Dunne,‡ R. Ent,‡ J.-O. Hansen,‡ D. Mack,‡ D. Meekins,‡ J. Mitchell,‡ S. Wood,‡ C. Yan,‡ Jae-Choon Yang,§ E. Belz,¶ E. Kinney,¶ D. van Westrum,¶ P. Markowitz,|| K. A. Assamagan,** O. K. Baker,**| K. Beard,** J. Cha,** T. Eden,** P. Gueye,** W. Hinton,** C. Keppel,** R. Madey,** G. Niculescu,** I. Niculescu,** L. Tang,** Wooyong Kim,†† C. Bochna,‡‡ H. Gao,‡‡ R. Holt,‡‡ M. Miller,‡‡ A. Nathan,‡‡ B. Terburg,‡‡ A. Ahmidouch,§§ R. Suleiman,§§ E. Bruins,¶¶ L. Kramer,¶¶ J. Martin,¶¶ A. Mateos,¶¶ R. Milner,¶¶ W. Kurchinetz,¶¶ C. Williamson,¶¶ W. Zhao,¶¶ E. Beise,|| || H. Breuer,|| || N. Chant,|| || F. Duncan,|| || J. J. Kelly, || || R. Mohring,|| || M. Khandaker,*** K. McFarlane,*** C. Salgado,*** S. Beedoe,†††S. Dangoulian,††† C. Jackson,††† D. Dutta,‡‡‡@ R. E. Segel,‡‡‡ Pat Welch,§§§ A. Klein,¶¶¶ S. Barrow,|| || || D. Beatty,|| || || H. T. Fortune,|| || || D. Koltenuk,|| || || W. Lorenzon,|| || || J. Yu,|| || || V. Frolov,**** J. Price|**** P. Stoler,**** R. Gilman,†††† J.-E.Ducret,‡‡‡‡ C. Cothran,§§§§ D. Day,§§§§ B. Zihlmann,§§§§ C. Armstrong, ¶¶¶¶ T. Amtuoni,|| || || || H. Mkrtchyan,|| || || || and V. Tadevosyan|| || || ||)

ANL led the first experiment to be carried out at TJNAF in 1995-1996. This experiment built upon earlier ANL work at MIT and SLAC using the (e,e'p) reaction to study the propagation of 0.35-3.3 GeV protons through nuclear material and the reaction mechanism in the quasifree region. The Hall C collaboration selected this experiment as one of the two commissioning experiments. Electrons were detected in the High Momentum Spectrometer and protons were detected in the Short Orbit Spectrometer except at the highest Q^2 setting where the roles of the spectrometers were reversed. The experiment utilized TJNAF beams of 0.845, 1.645, 2.445, and 3.245 GeV with up to 50 μA intensity on targets of C, Fe and Au. Hydrogen targets were used to check the normalization at each kinematic setting. Full commissioning studies of each spectrometer were performed to calibrate this experiment and to serve as a baseline for future experiments.

Measurements were made at Q^2 values of 0.64, 1.3, 1.8 and 3.3 $(GeV/c)^2$ corresponding to average proton kinetic energies of 0.35, 0.70,0.97 and 1.8 GeV to span the threshold for pion production in p-p collisions where the nature of the p-p cross section changes from dominantly elastic to dominantly inelastic. At Q^2 of 0.64 and 1.8 $(GeV/c)^2$ data were taken at two values of the virtual photon polarization to examine the separate contributions of longitudinal and transverse photon exchange. In all aspects the experimental performed as expected. The statistics, kinematic coverage and experimental precision significantly exceed those of previous measurements. This data set provides precise measurements of nuclear transparency as well as a broad survey of nuclear spectral functions from recoil momentum of 0 to 300 MeV and missing energy of 0 to 150 MeV.

The measurements of the average nuclear transparency were published in 1998. Radiatively corrected spectral functions have been extracted for each target and momentum transfer. These spectral functions suggest that the widths of deeply bound hole states in Fe and Au may be somewhat larger than had been expected. Figure IV-1 shows the results of the separation of the longitudinal and transverse spectral functions on carbon for missing momenta from 0 to 80 MeV at the two momentum transfers and the difference between the transverse and longitudinal strength at Q^2 of 0.6 and the difference in the transverse strength at the two Q^2. The longitudinal and transverse spectral functions of the p-shell knockout strength are consistent with each other. There is a substantial excess of transverse strength compared to the longitudinal strength in the missing energy region from 30-50 MeV at Q^2 of 0.6 $(GeV/c)^2$ (bottom panel of Fig. IV-1). At 1.8 $(GeV/c)^2$, the transverse strength is reduced (middle panel). Similar results are observed for iron and gold. The missing energy and nucleus dependence suggest that meson exchange mechanisms are important for the transverse strength, especially at the lower Q^2. The longitudinal strength is observed to extend to the highest missing

energies measured signaling the effects of short range correlations.

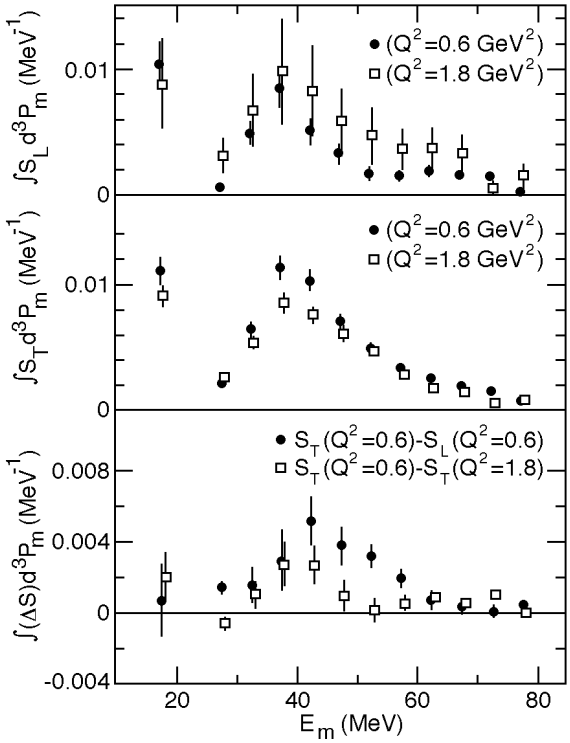

Fig. IV-1. The integrals of S_L (top panel) and S_T (middle panel) from $0<p_m<80$ MeV are shown at Q^2 of 0.64 (circles) and 1.8 $(GeV/c)^2$ (squares). In the bottom panel the differences: $S_T - S_L$ at 0.64 $(GeV/c)^2$ (circles) and $S_T(Q^2=0.6) - S_T(Q^2=1.8)$ (open squares) are shown. The errors are the sum in quadrature of the statistical and systematic uncertainties. The lowest E_m point is an average over $10 < E_m < 25$ MeV. The response functions at 1.8 $(GeV/c)^2$ are corrected for differences in proton attenuation by factors of 1.075 for $E_m < 25$ MeV and 1.18 for $E_m > 25$ MeV.

*American University; †Caltech; ‡TJNAF; §Chungnam National University, Taejon, Korea; ¶University of Colorado; ||Florida International University; **Hampton University; ††Kyungpook National University, Taegu, S. Korea; ‡‡University of Illinois, Urbana; §§Kent State University; ¶¶MIT; || ||University of Maryland; ***Norfolk State University; †††North Carolina A&T University; ‡‡‡Northwestern University; §§§Oregon State University; ¶¶¶Old Dominion University; || || ||University of Pennsylvania; ****Rensselaer Polytechnic Institute; ††††Rutgers University; ‡‡‡‡CE Saclay, France; §§§§University of Virginia; ¶¶¶¶William and Mary; || || || ||Yerevan Physics Institute, Armenia; @This experiment formed the basis for the Ph.D. theses of these students.

a.2. Electroproduction of Kaons and Light Hypernuclei

(J. Arrington, K. Bailey, F. Dohrmann, D. F. Geesaman, K. Hafidi, H. E. Jackson, B. Mueller, T. G. O'Neill, D. Potterveld, P. Reimer, J. P. Schiffer, B. Zeidman, and E91-016 Collaboration

Jefferson Lab experiment E91-016, "Electroproduction of Kaons and Light Hypernuclei" is a study of quasifree production of Kaons on targets of H, D, ^{3}He, and ^{4}He at an incident electron energy of 3.245 GeV. For H and D targets, data were also obtained at E_e =2.445 GeV. The scattered electron and emergent K^+ were detected in coincidence with the use of the HMS and SOS spectrometers, respectively, in Hall C. Angular distributions for the (e,e'K^+)Y reactions were measured at forward angles with respect to the virtual photon for Q^2 = 0.34, 0.37, and 0.5(GeV)^2. Particle identification utilizing time-of-flight detectors together with Aerogel Cerenkov detectors yields clean missing mass spectra, e.g. Report ANL/99-12, Fig III-6, and allows subtraction of random backgrounds. The experiment was run in two time periods. The H and D targets were studied over a period of months near the end of CY 1996 while the balance of the experiment, namely the ^{3,4}He targets were investigated during the last few months of CY 1999.

The fundamental interaction being studied is N(e,e'K^+)Y where Y is either a Λ or Σ and N represents a nucleon. For the H target, the final state can only be a Λ or Σ, but for heavier targets, there is relative motion between the nucleons in the target that results in broadening of the peaks. For the D target, it is possible to separate the two peaks inasmuch as the Fermi broadening is not large compared to the mass difference between Λ and Σ. For ^{3}He and ^{4}He, very preliminary missing mass spectra being shown in Fig. IV-2, it will be much more difficult to separate the yields for the various final states. Even in this very early stage of analysis, it is quite clear that the widths of the quasifree peaks are greater in ^{4}He than in ^{3}He (more binding and larger Fermi momenta).

For D, it is known that there is no bound Lambda-nucleon state, but for both ^{3}He and ^{4}He targets we anticipate bound hypernuclear states. Although the data shown in the figure are quite preliminary, it appears that bound Λ hypernuclear states are indeed seen. The possibility of bound Sigma hyper-nuclei also exists, but it is conjectural at this time. Construction of an optimal Monte Carlo simulation will require considerably more effort before any conclusions can be drawn. The large number of final state configurations results in complications that must be analyzed prior to extracting final cross sections. The present data set provides a high-statistics study of the mass dependence of Kaon electroproduction on light nuclei. There are a number of issues that must be investigated in the near future. Students from Hampton University and the University of Pennsylvania utilize data from E91-016 for their Ph.D. Theses.

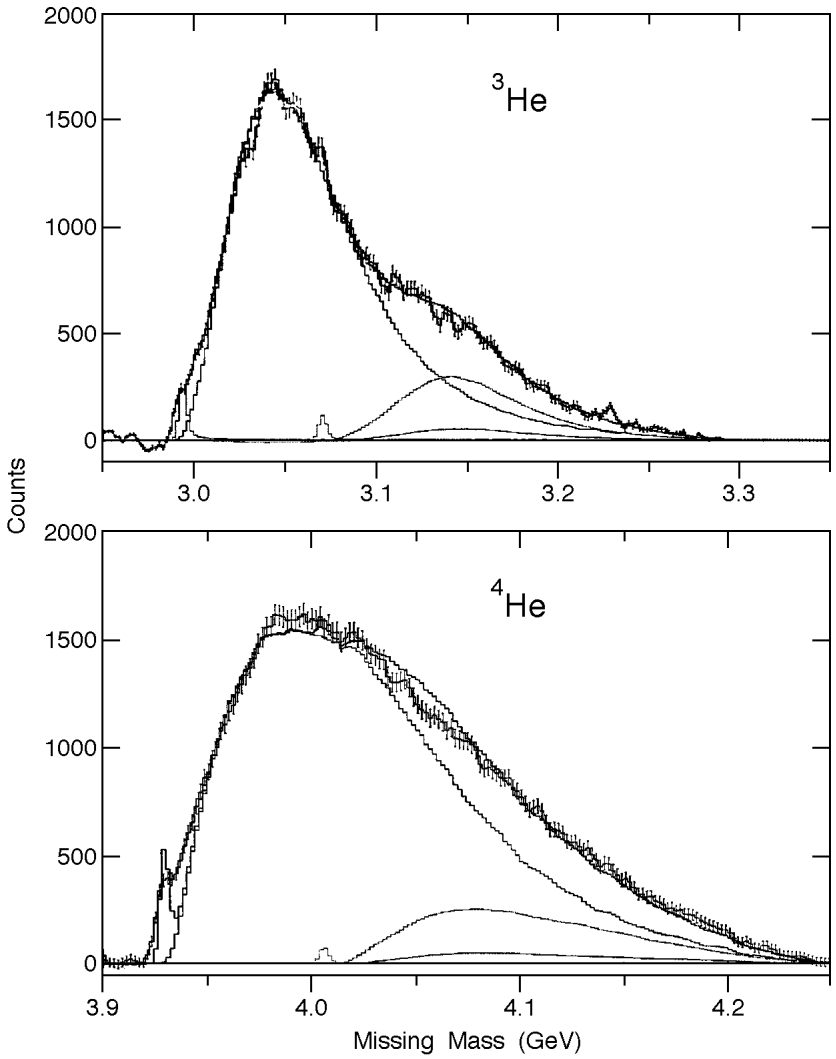

Fig. IV-2. Preliminary missing mass spectra for ^{3}He and ^{4}He(e,e'K$^+$) reactions. The broad curves that represent Monte-Carlo simulations for quasi-free production of Λ, Σ^0, Σ^- in decreasing magnitude respectively, are preliminary and relatively crude. The locations of possible "bound Λ and Σ states" are indicated by the narrow peaks (~ 5 MeV width and arbitrary magnitudes). The sums of the various contributions are also shown. It should be emphasized that it is very early and much analysis is required.

a.3. A Study of Longitudinal Charged-Pion Electroproduction in D, ^{3}He, and ^{4}He

(H. E. Jackson, J. Arrington, K. Bailey, D. De Schepper, D. Gaskell, D. F. Geesaman, B. Mueller, T. G. O'Neill, D. H. Potterveld, J. Reinhold, B. Zeidman, and the E91-003 Collaboration)

According to the simplest models of the nucleon-nucleon force, pion-exchange currents in nuclei should give rise to mass-dependent enhancement of the nuclear pion charge distribution. Longitudinal pion electroproduction should be a clean direct probe of the nuclear pion currents because of the dominance of the pion-pole process for charged-pion emission in the direction of the virtual photon. If current conceptions of pion-exchange currents in nuclei are correct, longitudinal electroproduction will be suppressed at lower momentum transfers and enhanced at higher momentum transfers. These currents should also manifest themselves in the quark-antiquark distribution functions as observed in deep-inelastic scattering on nuclei. However, analysis of parton distribution functions show no evidence for any mass enhancements of the sea quarks. Recent data from Drell-Yan studies which probe directly the quark-antiquark sea, show no mass dependence. These results, suggest that a reformulation of pion-exchange models of the medium- and short-range properties of nuclear forces may be required. In an attempt to probe exchange currents directly, we carried out a series of measurements of single-charged-pion electroproduction on the proton, deuteron, and ^{3}He at the TJNAF. The goal is to measure the longitudinal cross section in parallel kinematics by means of a Rosenbluth separation, and to search for target-mass dependent effects. The results from these measurements should provide insight into the absence of any enhancement of sea quark distributions in nuclei as measured in deep-inelastic scattering.

The measurements were carried out at Jefferson Lab in February-April 1998 using the Hall C facility. 0.845 to 3.245 GeV electrons were scattered from high-density cryo-targets. The scattered electrons were observed in the High Momentum Spectrometer in coincidence with pions observed in a short orbit spectrometer. The kinematic conditions corresponded to momentum transfers for which, in one case, the electroproduction is expected to be quenched, and a second, in which according to the standard pion-exchange model of nuclear forces, one expects a substantial enhancement. Measurements were made at kinematics corresponding to two virtual photon polarizations for each momentum transfer in order to use the data to carry out a Rosenbluth separation of the transverse and longitudinal cross sections. To date, measurements have been made for the proton, deuterium, and ^{3}He. A direct comparison of the cross sections for each target measured in the identical geometry will allow the determination of mass dependencies without measurements of absolute cross sections. The data analysis has been focused on careful simulations of the spectrometer acceptances, as well as other relevant instrumental effects. Monte Carlo distributions have been generated using the Hall C simulation, SIMC, which includes spectrometer acceptance, radiative processes, energy loss, and particle decay. The measured cross sections are established by comparing the results of the SIMC simulations to data with a hypothesied input cross section and then iterating until agreement with the data is achieved. The general features of the deuterium and ^{3}He pion spectra in missing mass, are typical of quasifree scattering. For the π^+ production on ^{3}He, in addition to the quasifree component which appears to be the same as for π^-, there is a sharp peak corresponding to coherent production leading to a triton in the final state, and a second component corresponding to a deuteron and neutron in the final state. Preliminary longitudinal-transverse separations have been reported and the analysis is being refined in order to obtain the maximum achievable accuracy for the longitudinal and transverse cross sections and their mass dependencies. To date, there is no evidence for any enhancement of the longitudinal cross sections above the quasifree values expected in a simple impulse approximation. Rather there appears to be substantial quenching, particularly in ^{3}He. Preliminary results, for the ratio of the observed cross sections to those expected from simple quasifree scattering are presented in Fig. IV-3. If an enhancement due to pion exchange currents were to occur, the effect would be expected to manifest itself in the region of virtual pion momenta near 400-500 MeV where we have an experimental point.

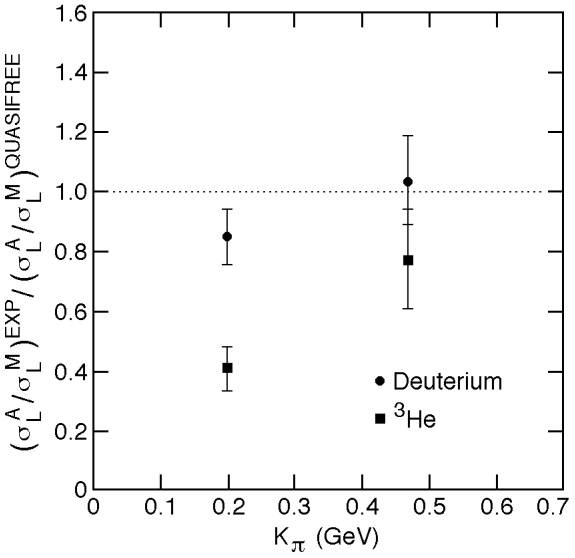

Fig. IV-3. Measured longitudinal cross section ratios for forward angle pion electroproduction on deuterium and ^{3}He corrected for kinematic effects induced by the quasifree scattering mechanism.

a.4. Pion Electroproduction from H_2 and D_2 at W=1.95 GeV (H. E. Jackson, J. Arrington, D. Gaskell, B. Mueller, and the E93-021 Collaboration)

The pion, as the lightest meson, is an ideal laboratory for studying the transition between the non-perturbative and perturbative regions of QCD. Experimental results for the value of the pion form factor, (F_π), at moderate and high Q^2 have large experimental uncertainties. Experiment E93-021 measured the H(e,e′π^+)n reaction at TJNAF for Q^2 values from 0.6-1.6 $(GeV/c)^2$. The forward longitudinal response in this process is dominated by the knockout of virtual pions, and is therefore sensitive to the pion form factor. Data analysis is in progress and is focused on obtaining longitudinal and transverse separated cross sections. The value of F_π at Q^2 of 0.6, 0.75, 1.0, and 1.6 $(GeV/c)^2$ will be obtained from this data. E93-021 has also measured the D(e,e′π^+)nn and D(e,e′π^-)pp reactions. The π/π^+ ratio is sensitive to contributions to the cross section which are unrelated to F_π The hydrogen and deuterium data samples from E93-021 is also being analyzed to determine the ratio of the longitudinal part of the π^+ electroproduction cross section from deuterium to that from hydrogen. This analysis is performed as part of the E91-003 experiment, and will provide complimentary information about the enhancement of the nucleon pion field at W=1.95 GeV and Q^2 from 0.6-1.6 $(GeV/c)^2$.

a.5. Measurements of Deuteron Photo-disintegration up to 5.5 GeV (D. F. Geesaman, H. E. Jackson, T. G. O'Neill, D. H. Potterveld, B. Zeidman, J. Arrington, B. Mueller, and the E89-012 and E96-003 collaborations)

Constituent-counting-rule behavior was observed previously in high energy proton-proton scattering and photo-meson productions from the proton. Only one nuclear reaction thus far has exhibited this behavior. Argonne experiments NE8 and NE17 at SLAC showed that the deuteron photodisintegration d(γ,p)n reaction at a proton center-of-mass angle of 90° starts to show the scaling behavior at the unexpectedly low photon energy of around 1.0 GeV. Extending the SLAC measurements to higher photon energies and performing a detailed angular distribution study is essential to identify the limits of the kinematic regime of this behavior and to investigate the underlying mechanisms.

TJNAF experiment E89-012, one of the two hall-C commissioning experiments performed in 1996,

measured for the first time the differential cross section for d(γ,p)n up to 4.0 GeV at center-of-mass angles 36°, 52°, 69°, and 89°. The d(γ,d) π° reaction was also studied at E_γ = 0.8-3.2 GeV. The d(γ,p)n results[1], shown in Fig. IV-4, are in good agreement with the previous measurements and the data near 90° continue to show the scaling behavior up to 4 GeV and are also in fair agreement with an asymptotic meson-exchange model calculation[2]. The data at 36° and 52° do not exhibit the counting-rule behavior, but also do not extend to as high a region of transverse momenta as the 90° data. The d(γ,d) π^0 results are consistent with previous measurements at low photon energy, but do not show any signs of scaling at a center-of-mass angle of 90°. In contrast, the results at 136° are in good agreement with the constituent-counting-rule behavior.

This work was continued in TJNAF experiment E96-003, which ran in the spring of 1999. The d(γ,p)n cross sections were measured for beam energies of 5.0 and 5.5 GeV, at center-of-mass angles of 37° (5 GeV only), 53°, and 70°. The higher energy of these measurements should provide a more stringent test of the theoretical models for this reaction. The analysis of these data is currently in progress.

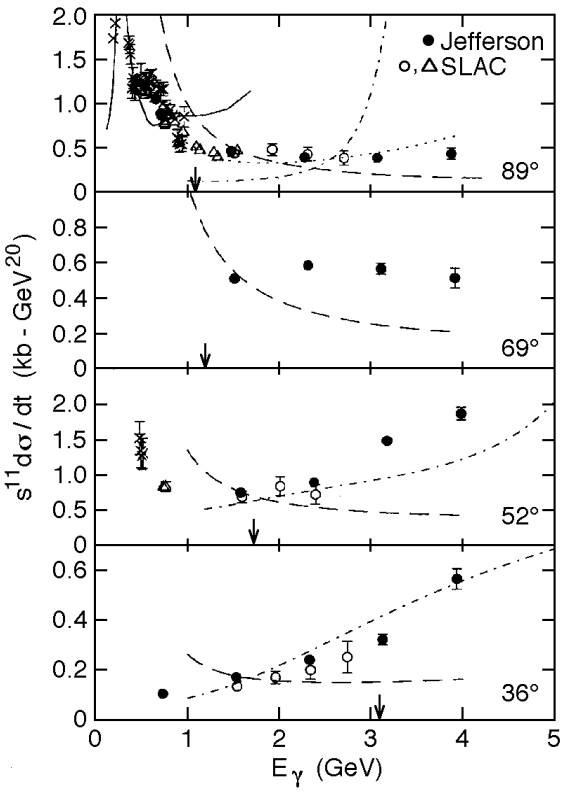

Figure IV-4. $s^{11}d\sigma/dt$ vs. E_γ for the d(γ,p)n reaction. The present work is shown as solid circles with statistical uncertainties only, the SLAC NE17 data are shown as open circles, the SLAC NE8 data are shown as open triangles, and other existing data are shown as crosses. The solid line is the meson-exchange model calculation of Lee[3]. The long-dashed line is the RNA analysis[4], and the dotted line is Nagornyi's[2] asymptotic meson-exchange calculation. The dash-dotted line is the QGS calculation[5]. The arrows indicate the photon energies where p_T^2 = 1.0 (GeV/c)^2. The previous data are shown above at nominal center of mass angles of 37°, 53°, and 90°.

[1] C.~Bochna *et al.*, Phys. Rev. Lett. **81**, 4576 (1998).
[2] S. I.~Nagornyi, Yu. A. Kasatikin, and I. K. Kirchenko, Sov. J. Nucl. Phys. **55** 189 (1992).
[3] T.-S. H. Lee, Argonne National Laboratory Report No. PHY-5253-TH-88; T.-S. H. Lee, in *Proceedings of the International Conference on Medium and High Energy Nuclear Physics, Taipei, Taiwan, 1988* (World Scientific, Singapore, 1988), p.563.
[4] S. J. Brodsky and J. R. Hiller, Phys. Rev. C **28**, 475 (1983).
[5] L. A. Kondratyuk *et al.*, Phys. Rev. C **48**, 2491 (1993).

a.6. HERMES, Measurements of Spin-Structure Functions and Semi-Inclusive Asymmetries for the Proton and Neutron at HERA (J. Arrington, H. E. Jackson, T. G. O'Neill, D. H. Potterveld, D. De Schepper, and collaborators at 33 other institutions)

Since 1995, the HERMES experiment has provided fundamental new insights into the structure of the nucleon, especially on the composition of its spin. The unique capabilities of the experiment have produced data that were not possible with previous measurements at SLAC, CERN, and Fermilab. The collaboration has collected and analyzed millions of deep-inelastic scattering (DIS) events using longitudinally polarized electrons and positrons incident on longitudinally polarized internal gas targets of ^{1}H, ^{2}H, and ^{3}He, as well as thicker unpolarized gas targets. These data together with large sets of photo-production events have yielded several results that were unexpected and are provoking new work, both theoretical and experimental. Thanks to the large momentum and solid angle acceptance of the HERMES spectrometer, these results extend well beyond the principal HERMES role of studying nucleon spin structure.

The HERMES collaboration consists of approximately 30 institutions from North America and both western and eastern Europe. The HERMES experiment is located in the East straight section of the HERA storage ring at the DESY laboratory in Hamburg. Positron (or electron) beam polarizations are stable and reproducible at about 50%, and are monitored with systematic uncertainties of better than ±5% by two independent Compton backscattering polarimeters. The 27.5 GeV longitudinally polarized lepton beam interacts with polarized internal gas targets stored in an open-ended thin-walled storage cell. Data were taken on a polarized ^{3}He target in 1995, on a polarized ^{1}H target in 1996 and 1997, and on a polarized ^{2}H target in 1998 and 1999. The target densities are about 7.5 (5) x 10^{13} atoms/cm^2 for hydrogen (deuterium) and 3.5 x 10^{14} atoms/cm^2 for ^{3}He. Typical polarizations of the target are 90% (50%) for the hydrogen/deuterium (^{3}He) sources, and are measured to better than ±5% with polarimeters. Luminosities are in the range of 4-30 x 10^{31} nucleons cm^{-2} sec^{-1}. Unpolarized gases of hydrogen, deuterium, nitrogen, and krypton, with thicknesses of around 10^{15} atoms/cm^2, are also used for data taking.

The experimental apparatus is an open-geometry forward spectrometer with momentum analysis and background rejection provided by a 1.3 T-m dipole magnet. The spectrometer is constructed in two symmetric halves above and below the positron ring plane. Forty-two drift chamber planes and 6 micro-strip gas chamber planes provide tracking in each spectrometer half. Particle identification is provided by the combination of a lead-glass calorimeter, a pre-shower detector consisting of a scintillator hodoscope preceded by 2 radiation lengths of lead, a transition radiation detector, and a threshold Cerenkov detector. The Cerenkov counter was upgraded to a ring imaging configuration in 1998 (see section a.11). A detailed description of the spectrometer is found in Ref. 1. The angular acceptance of the experiment is $40 < \Theta < 220$ mrad. The kinematic range accessible is $0.02 < x < 0.8$ and $0.2 < Q^2 < 20$ (GeV/c)^2. Argonne provided the Cerenkov counter used for particle identification, led the RICH upgrade effort, and developed the drifilm coating technique for the ultrathin target cell required for this experiment.

HERMES has performed a measurement of the flavor asymmetry between up and down quarks in the nucleon sea[2], several studies of fragmentation of up and down quarks to pions, measurement of the DIS contributions to the generalized Gerasimov-Drell-Hearn integral for both the proton and neutron[3], a measurement of the spin transfer from virtual photons to Λ^0 hyperons, measurements of the effect of the nuclear environment on the hadronization process to study its time development, and most recently the observation at small Q^2 of a surprisingly large difference in the effects of the nuclear medium on the transverse and longitudinal DIS cross sections[4]. (Here $-Q^2 = q^2$ is the square of the invariant mass of the exchanged virtual photon, a measure of the resolution of the probe.) A broad program of measurements involving diffractive vector meson production is also underway with basic studies in ρ^0, φ^0, ω^0, and J/Ψ production, as well as the determination of photon → vector-meson spin density matrix elements through the analysis of the angular distribution of the decay products[5]. The ρ^0 semi-exclusive cross section has been found to have a large and unexpected spin dependence[6]. The study of diffractive ρ^0 production in nuclei has led to the observation of a lifetime (coherence length) effect on the initial-state nuclear interactions of the virtual quark pair that represent the hadronic structure of the photon[7].

The spin-dependence of inclusive DIS lepton scattering has been used by HERMES and other experiments to

provide information about the total contribution of all quark species to the nucleon spin. Much more detailed information about the spin content of the nucleon can be obtained from the spin-dependence of the semi-inclusive deep inelastic scattering (SIDIS) reaction, $eN \rightarrow eh^{\pm}X$. (Here $h^{\pm}$ refers to a positive or negative hadron detected in coincidence with the scattered positron.) In the quark parton model, the factorization approximation relates the detected hadron to the struck quark. In this approximation, the asymmetries measured in inclusive and semi-inclusive DIS can be combined to extract the contribution of each quark flavor q (=up, down, or strange) to the nucleon spin, and to distinguish between the contributions of valence and sea quarks. Figure IV-5 exhibits the polarized distribution functions of valence and sea quarks measured at

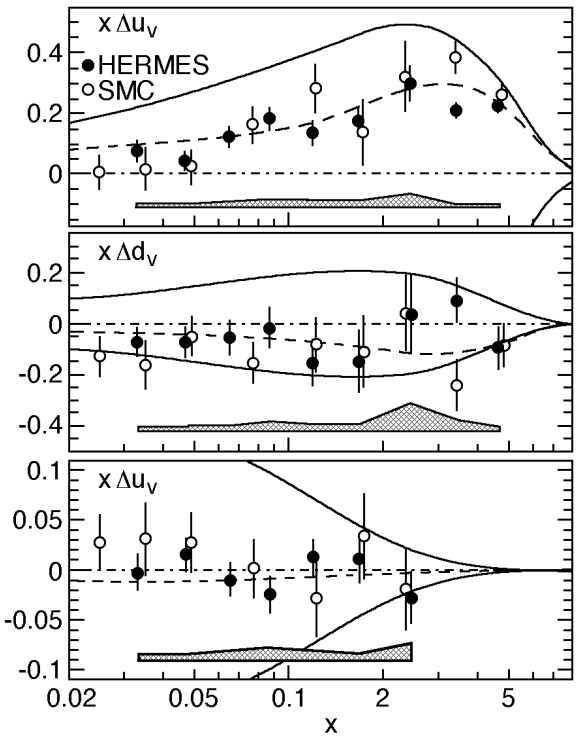

Fig. IV-5. The polarized valence and sea quark distributions measured at HERMES (1995-1997) and SMC (all data).

HERMES and SMC. In the figure, $\Delta q(x) = q^{+}(x) - q^{-}(x)$ where $q^{+}(x)$ $[q^{-}(x)]$ is the probability of finding a quark of flavor q in a proton with spin oriented parallel (antiparallel) to the proton and carrying a fraction x of the proton's momentum in the infinite momentum frame. The valence contribution $\Delta q_v(x) = \Delta q(x) - \Delta^{-} q(x)$ is found by subtracting the sea contribution $\Delta^{-} q(x)$ from the distribution function for each flavor. (Here ^{-}q refers to the antiquark of flavor q.) The HERMES results substantially improve the knowledge of the polarized parton distributions, especially on $\Delta u_v(x)$ and on the polarization of the sea quarks. The deuterium data being acquired in 1999/2000 will allow nearly as precise a determination of Δd_v. In addition the addition of the RICH detector in 1998 will allow the first measurement of the separate SIDIS asymmetries for the different hadron species (pions, kaons, and protons)--see section a.11. This will greatly improve the determination of the polarization of the different quark flavors, especially of the strange quark, whose polarization is presently weakly constrained.

The precise inclusive and semi-inclusive polarized deep-inelastic scattering data from SLAC, CERN and HERMES clearly show that the quark spins account for only about 20% of the nucleon's spin. Much of the remainder could be provided by a possible large positive polarization of the gluon field in the proton. It is important to test this hypothesis by measuring the gluon helicity distribution, $\Delta G(x)$. Phenomenogical LO QCD fits to the scaling violations observed in the polarized structure function $g_1(x,Q^2)$ suggest that the integral of $\Delta G(x)$ is positive, but some theoretical models predict a negative contribution to the nucleon spin[8]. Lepto-production reactions dominated by the direct coupling of the exchanged virtual photon to one of the gluons in the nucleon, a process known as photon-gluon fusion (PGF), allow more direct measurement of $\Delta G(x)$ because the gluon distribution enters in leading order. Monte Carlo studies indicate that in the HERMES experiment, PGF dominates the photo-production of pairs of hadrons with opposite charge and high transverse momentum. If so, the beam-target spin asymmetry can be used to determine the polarization of the glue because the PGF process has a strong negative polarization analyzing power.

For h^{+} h^{-} pairs where one hadron has a transverse momentum of at least 1.5 GeV/c and the other of at least 1.0 GeV/c, the asymmetry is found to be $A_{\parallel} = -0.28 \pm 0.12$ (stat) ± 0.02 (syst). Given the Monte Carlo prediction of PGF dominance, this indicates a significant *positive* polarization of the gluons. The negative value supports the Monte Carlo prediction, since none of the known background processes exhibit negative asymmetries (deep-inelastic scattering from protons is characterized by positive asymmetries). A leading order QCD model was implemented in the PYTHIA Monte Carlo generator to determine the effect on the asymmetry of the background processes, such as

the QCD Compton effect. Within the context of this model, the measured asymmetry implies a value $\Delta G(x)/G(x)$ of 0.41 ±0.18 ±0.03 for the fractional polarization of gluons with momentum fraction $\langle x_G \rangle$ = 0.17. The value is consistent with the phenomenological fits to the $g_1(x,Q^2)$ scaling violations. The contribution to the HERMES measurement from model uncertainty is unknown, and the Monte Carlo underpredicts by a factor of two the yield of hadron pairs with high transverse momentum. Nevertheless, in the absence of other sources of negative asymmetry, the data indicate that the glue is positively polarized.

HERMES has just begun to demonstrate the quality and variety of the results it can obtain. Results are being developed and finalized on many additional topics, and present and future running will greatly improve the statistical precision of the results already shown. Moreover, the HERMES apparatus has recently been upgraded and improved: a reduction in the diameter of the target storage tube has led to a 50% increase in the luminosity; a dual-radiator RICH has replaced the threshold Cerenkov counter, allowing identification of pions, kaons and protons over nearly the entire momentum acceptance of the detector (see section a.11); an instrumented iron wall was built, which enables the identification of muons; a wheel-shaped array of silicon counters is being installed just downstream of the target such that the acceptance for Λ^0 hyperons and J/Ψ mesons (in conjunction with new wide-angle scintillators behind the magnet) is increased by a factor of 4; a new set of quadrupoles behind the experiment is being equipped with tracking chambers between their pole faces that make it possible to reconstruct the virtual-photon energy ν for some of the photo-produced J/Ψ mesons. Furthermore, preparations are being made for the installation (in the first months of 2001) of a new silicon recoil detector below the target. Coupled with recent improvements in the HERA electron (or positron) beam current, these improvements will help lead to a rich future of HERMES physics results.

---

[1]HERMES, K. Ackerstaff *et al.*. "The HERMES Spectrometer", Nucl. Instr. & Meth. A **417**, 230 (1998).
[2]HERMES, K. Ackerstaff *et al.*. "The Flavor Asymmetry of the Light Quark Sea from Semi-inclusive Deep Inelastic Scattering", Phys. Rev. Lett. **81**, 5519 (1998).
[3]HERMES, K. Ackerstaff *et al.* "Determination of the Deep-Inelastic Contribution to the Generalized Gerasimov-Drell-Hearn Integral for the Proton and Neutron", Phys. Lett. B **444**, 531 (1998).
[4]HERMES, K. Ackerstaff *et al.* "Nuclear Effects on $R\sigma_L/\sigma_T$ in Deep-Inelastic Scattering", DESY 99-150, hep-ex/9910071, Phys. Lett. (in press).
[5]HERMES, K. Ackerstaff *et al.* "Measurement of Angular Distributions and $R= \sigma_L/\sigma_T$ in Diffractive Electroproduction of ρ^0 Mesons",
DESY 99-199.
[6]F. Meissner, "Double-Spin Asymmetry in Exclusive Vector Meson Production at HERMES", Proceedings of the 7th Int. Workshop on Deep Inelastic Scattering and QCD, DIS99, Zeuthen, Germany, April 1999, DESY HERMES 99-028.
[7]HERMES, K. Ackerstaff *et al.* "Observation of a Coherence Length Effect in Exclusive ρ^0 Electroproduction", Phys. Rev. Lett. **82**, 3025 (1999).
[8]R. L. Jaffe, Phys. Lett. B **365**, 359 (1996).

a.7. Results from Exclusive, Diffractive ρ^0 Electroproduction (T. G. O'Neill, J. Arrington, D. De Schepper, H. E. Jackson, D. H. Potterveld, and collaborators at 33 other institutions)

A signal for the exclusive electroproduction of the neutral $\rho(770)$ meson was isolated as a subset of the standard HERMES deep inelastic scattering data. In this reaction, the electron or positron emits a virtual photon which then fluctuates into a quark-antiquark pair of lifetime l_c. A diffractive interaction with the target converts the quark-antiquark pair into the detected ρ^0. The ρ^0 meson, which decays into 2 pions, manifests itself in a peak at $M_\rho = 0.77$ GeV in the invariant mass of the 2-pion system. Energy and momentum conservation can be used to ensure that there are no additional particles in the final state, resulting in a clean signal for the exclusive $eN \rightarrow e\,\rho^0\,N$ reaction. Measurements of the reaction inside nuclei have confirmed that the lifetime of the quark-antiquark fluctuation is correctly given by l_c, and that it interacts with the nucleus like a physical ρ^0 meson[1]. Publications are being finalized on the unpolarized ρ^0 production cross section and on the $\rho^0 \rightarrow \pi^+ \pi^-$ decay angular distributions[2]. The cross section results will help illuminate the transition in the ρ production reaction mechanism from the low- to high-energy regimes, and constrain novel theories of the reaction in terms of off-forward parton distributions. The decay results provide unprecedented detail about the helicity structure of the reaction at HERMES energies. This information is complemented by the first observation of a non-trivial dependence of a vector meson production reaction on the relative orientation of beam and target spins[3], see Fig. IV-6. The discovery is especially interesting in the context of a preliminary SMC result showing no such dependence in ρ production at higher energy, where the reaction is dominated by exchange of the (presumably) spinless pomeron. The HERMES result suggests a violation of s-channel helicity conservation, which is approximately observed in diffractive reactions. It also casts new light onto the production of the ρ^0 by transverse photons which, unlike production by longitudinal photons, cannot presently be calculated in the context of perturbative QCD.

[1] HERMES, K. Ackerstaff *et al.* "Observation of a Coherence Length Effect in Exclusive ρ^0 Electroproduction", Phys. Rev. Lett. **82**, 3025 (1999).

[2] HERMES, K. Ackerstaff *et al.* "Measurement of Angular Distributions and $R = \sigma_L/\sigma_T$ in Diffractive Electroproduction of ρ^0 Mesons", DESY 99-199.

[3] F. Meissner, "Double-Spin Asymmetry in Exclusive Vector Meson Production at HERMES", Proceedings of the 7th Int. Workshop on Deep Inelastic Scattering and QCD, DIS99, Zeuthen, Germany, April 1999, DESY HERMES 99-028.

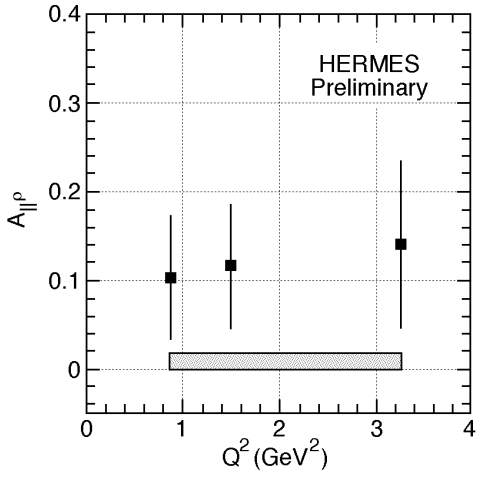

Fig. IV-6. Longitudinal beam-target asymmetry $A_{||}^{\rho}$ (fractional dependence of the cross section on relative beam-target spin orientation) for exclusive ρ^0 production as a function of Q^2, with a systematic uncertainty band.

a.8. Measurements of Inclusive Cross Section and R = σ_L/σ_T in The Nucleon Resonance Region

(J. Arrington, D. F. Geesaman, H. Gao, T. G. O'Neill, D. Potterveld, J. Reinhold, C. Keppel,* K. Assamagan,* O. K. Baker,* W. W. Buck,* A. Cochran,* L. Gan,* A. Gasparian,* R. Green,* P. Gueye,* I. Niculescu,* E. Segbefia,* L. Tang,* C. Williams,* L. Yuan,* P. Bosted,† S. Rock,† B.D. Anderson,‡ G. Petratos,‡ J.W. Watson,‡ W. M. Zhang,‡ W. Lorenzon,§ J. Dunne,¶ S. Beedoe,|| S. Danagoulian,|| C. Jackson,|| R. Sawafta,|| V. V. Frolov,** J. Napolitano,** J. Price,** P. Stoler,** C. Armstrong,†† R. Carlini,†† R. Ent,†† K. Garrow,†† J. Gomez,†† A. Lung,†† D. Mack,†† J. H. Mitchell,†† A. Saha,†† W. Vulcan,†† S. Wood,†† C. Yan,†† C. Cothran,‡‡ D. Day,‡‡ M. Zeier,‡‡ B. Zihlmann,‡‡ H. P. Blok,§§ H. Mkrtchyan,¶¶ Ts. Amatuni,¶¶ V. Tadevosian,¶¶ D. Beck,|| || C. W. Bochna,|| || R. J. Holt,|| || M. A. Miller,|| || B. P. Terburg,|| ||D. Dutta,*** R. E. Segal,*** B. W. Filippone,††† E. Kinney,‡‡‡ D. van Westrum,‡‡‡ D. M. Koltenuk,§§§ and R. M. Mohring¶¶¶)

Reliable global descriptions of inclusive electroproduction data are necessary for electron-nucleon scattering model development, accurate radiative correction calculations, and the extraction of form factors, structure functions, and parton distribution functions from inclusive electron scattering experiments.

A great deal of our understanding of the quark structure of the nucleon comes from inclusive electron scattering. However, most of the measurements focus on the deep inelastic region. High precision cross section measurements in the resonance region, combined with a separation of the longitudinal (σ_L) and transverse (σ_T) components, will substantially improve the global description of electroproduction at moderate to high Q^2 and large Bjorken-x. Measurements have been made to extract the ratio $R= \sigma_L/\sigma_T$ from deep inelastic cross sections at momentum transfers as high as $Q^2 = 50$ $(GeV/c)^2$, and from elastic electron-proton scattering up to $Q^2 = 8.83$ $(GeV/c)^2$. In contrast to both the elastic and the deep inelastic, there exist few separation measurements of the ratio R in the resonance region at moderate or high momentum transfers.

A series of measurements of inclusive electron scattering in the resonance region was taken during in Hall C at Jefferson Lab during 1995 and 1996 running. Data were obtained from both hydrogen and deuterium allowing extraction of the resonance production cross section from both the proton and the neutron. The cross sections were measured for momentum transfers between 0.5 and 5.0 $(GeV/c)^2$. Generating interest recently is an observed scaling relationship between resonance electroproduction and deep inelastic scattering, termed local duality. First observed by Bloom and Gilman, this duality suggests a common origin for both kinematic regimes. Local duality was observed both for the entire region and locally in the vicinity of each prominent resonance. In addition, the structure functions measured appear to be insensitive to sea quarks, giving a scaling curve that represents the valence quark distribution of the nucleon. Theoretical models indicate that both the longitudinal and the transverse structure functions should manifest Bloom-Gilman duality, but previous experiments that separated the longitudinal and transverse components did not have the precision necessary to study duality. A fundamental quark description of nucleons may be expanded to include information in the resonance region by studying duality with new resonance electroproduction data and better measurements of $R = \sigma_L/\sigma_T$. In 1999, experiment E94-110 was run in Hall C at Jefferson Lab. The experiment made a precision measurement of R in the resonance region, up to $Q^2= 7.5$ $(GeV/c)^2$. This new data should reduce the uncertainty in R from greater than 100% to approximately 10%. There is also an additional approved experiment to extend duality studies to higher Q^2, and a proposal has been submitted to the Jefferson Lab PAC to make additional measurements at low x and Q^2. The goal of this proposal is to more carefully examine the valence sensitivity of the data and to examine the low Q^2 evolution of the structure functions.

*Hampton University; †The American University; ‡Kent State University; §University of Michigan; ¶Mississippi State University; || North Carolina A&T University; **Rensselaer Polytechnic Institute; ††Thomas Jefferson National Accelerator Facility; ‡‡University of Virginia; §§Vrije Universiteit; ¶¶Yerevan Physics Institute; || ||University of Illinois; ***Northwestern University; †††California Institute of Technology; ‡‡‡University of Colorado; §§§University of Pennsylvania; ¶¶¶University of Maryland

a.9. Measurements of the Nuclear Dependence of $R = \sigma_L/\sigma_T$ at Low Q^2

(J. Arrington, D. F. Geesaman, T. G. O'Neill, D. Potterveld, O. K. Baker,* A. Cochran,* L. Gan,* A. Gasparian,* T. Green,* P. Gueye,* B. Hu,* A. Johnson,* A. E. Keppel,* E. Segbefia,* L. Tang,* A. Bruell,† K. McIlhany,† R. G. Milner,† T. Shin,† J. Dunne,‡ R. B. Piercey,‡ C. S. Armstrong,§ R. Carlini,§ R. Ent,§ H. C. Fenker,§ K. Garrow,§ J. Gomez,§ A. Lung,§ D. Mack,§ J. H. Mitchell,§ W. F. Vulcan,§ S. A. Wood,§ E. Kinney,¶ B. van der Steenhoven,|| B. Blok,** B. Zihlmann,** W. Lorenzon,†† B. Filippone,‡‡ and J. Martin‡‡)

Inclusive electron scattering is a well understood probe of the partonic structure of nucleons and nuclei. Deep inelastic scattering has been used to make precise measurements of nuclear structure functions over a wide range in x and Q^2. The ratio $R = \sigma_L/\sigma_T$ has been measured reasonably well in deep inelastic scattering at moderate and high Q^2 using hydrogen and deuterium targets. However, R is still one of the most poorly understood quantities measured in deep inelastic scattering and few measurements exist at low Q^2 or for nuclear targets. Existing data at moderate to large values of Q^2 rule out significant nuclear effects in R. However, evidence for substantial A-dependent effects has been recently reported by the HERMES collaboration at low x and Q^2. Figure IV-7 shows the ratio R_A/R_D for ^{3}He and Nitrogen, along with values extracted from NMC and SLAC data. While HERMES can not directly measure R (which requires data at multiple beam energies), they do measure the ratio of R_A to R_D. They see a significant deviation from unity in the ratio of $R_{^3He}/R_D$ and R_N/R_D for x = 0.05 and Q^2 = 2.0.

Jefferson Lab Experiment E99-119 is a direct measurement of R at low x (down to x = 0.02) and low Q^2 (down to 0.07 $(GeV/c)^2$). The measurement will be made on hydrogen, deuterium, and several nuclear targets (up to A=197). This will both significantly improve the measurement of R at low Q^2 for the proton, and examine the nuclear dependence of R in the region where the HERMES experiments has seen the A-dependence. Experiment E99-119 has been tentatively scheduled to run in Hall C in the summer of 2000.

*Hampton University; †Massachusettes Institute of Technology; ‡University of Colorado; §Thomas Jefferson National Accelerator Facility; ¶Mississippi State University; || NIKHEV; ** Vrije Universiteit Amsterdam; ††University of Michigan; ‡‡California Institute of Technology

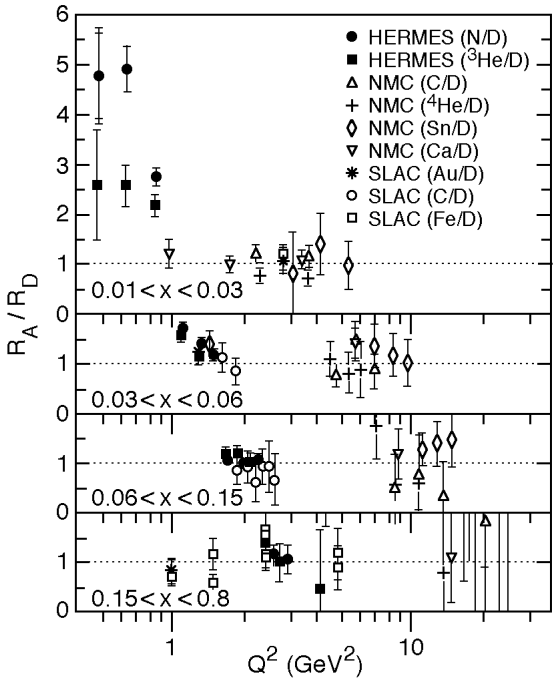

Fig. IV-7. The ratio of R_A to R_D as a function of Q^2 for four bins in x. Previous data from NMC and CLAC are consistent with one. The new HERMES data are consistent with the previous measurements, but show a significant deviation from unity for low values of x and Q^2.

a.10. Momentum Transfer Dependence of H(e,e'K$^+$)Y Reactions (J. Arrington, K. Bailey, D. F. Geesaman, H. E. Jackson, T. G. O'Neill, D. Potterveld, J. Reinhold, J. P. Schiffer, B. Zeidman, and E93-18 Collaboration)

In Jefferson Lab experiment E93-18, the momentum transfer dependence of the reaction H(e,e'K$^+$)Y, where Y is Λ or Σ^0, was studied at Q^2 = 0.5, 1.0, 1.5, and 2.0 $(GeV/c)^2$ at incident electron energies ranging from 2.445 to 4.045 GeV. The HMS and SOS spectrometers in Hall C were used for detection of the emergent electrons and K^+, respectively. For each Q^2, data were obtained at three different values of the polarization of the virtual photon in order to separate the longitudinal and transverse parts of the cross section. Together with data on the neutron (E91-16), this study is vital for understanding processes that lead to production of bound hypernuclei. Students from Hampton University[1] and the University of Maryland[2] utilized data from E93-18 for doctoral theses.

For Λ production, the ratio, $R = \sigma_L/\sigma_T$, was found to reach a maximum ≈1 at Q^2 = 0.75 $(GeV/c)^2$. The data were compared to calculations and provide significant constraints on theoretical models. These results were published.[3] The data for Σ^0 production agree with previous results for unpolarized cross actions as a function of Q^2 and with increasing Q^2, R decreases from a value ≈2 at Q^2 ≈ 0.5. Comparison with theoretical models is in progress.

[1] G. Niculescu, Ph.D. Thesis-Hampton University (1998)
[2] R. M. Mohring, Ph.D. Thesis-University of Maryland (1999)
[3] G. Niculescu *et al.*, Phys. Rev. Lett. **81**, 1805 (1998)

a.11. A Dual Radiator Ring Imaging Cerenkov Counter for HERMES

(H. E. Jackson, K. G. Bailey, D. M. De Schepper, T. P. O'Connor, T. G. O'Neill, D. H. Potterveld, J.-O. Hansen,* R. S. Kowalczyk,† and the HERMES Collaboration)

The HERMES experiment is unique among contemporary experimental studies of the spin structure of the nucleon in its emphasis on unambiguous measurement of pion, kaon, and nucleon semi-inclusive spin asymmetries in deep-inelastic scattering. These asymmetries provide information for the study of the flavor dependence of polarized structure functions and of the sea polarization. However, most of the hadrons produced in HERMES lie between 2 and 10 GeV, a region in which it has not been feasible to separate pions, kaons, and nucleons with standard PID techniques. RICH and threshold Cerenkov systems using heavy gases such as C_4F_{10}, at atmospheric pressure are useful only for energies above 10 GeV since the kaon threshold for Cerenkov radiation is typically higher than 9 GeV. Use of a high-pressure gas system is not technically feasible in HERMES. Clear liquid radiators are useful for hadron identification below roughly 2 GeV because of their correspondingly very low Cerenkov light thresholds.

To overcome these difficulties, the HERMES collaboration has replaced the existing threshold Cerenkov counters in the HERMES spectrometer with a dual-radiator RING Imaging Cerenkov Counter (RICH) which employs a new technology. The detector was designed and built by a collaboration of 8 institutions, led by Argonne (Argonne, Bari, CalTech, Frascati, Gent, Rome, Tokyo, and Zeuthen), in 12 months from concept to installation. The installation of the RICH was completed on 22 May, 1998 and has been commissioned during the past year. It is the first use of recently developed clear, hydrophobic aerogel as a Cerenkov radiator in a RICH system. In order to identify almost all of the pions, kaons and protons in the HERMES acceptance, the RICH is filled with a second radiator (C_4F_{10} gas) which in combination with the aerogel, provides complete hadron identification from 2 GeV/c to about 15 GeV/c. The basic geometry and radiator configuration are shown in Fig. IV-8. Rings from the aerogel (n = 1.03) provide identification up to about 9 GeV/c, while rings from the gas (n = 1.0015) are used for higher momenta. The RICH actually consists of a pair of identical counters, one in the upper half and second in the lower half of the HERMES spectrometer. Each photon detector is an array of 1934 3/4" photomultipliers arranged in a planar array of honeycomb packing. For a fully realistic particle, a typical ring pattern consists of a small inner ring generated by photons from the gas and a larger concentric ring of hits generated by photons from the aerogel. The ring pattern for a sample event is shown in Fig. IV-9.

The detector has operated routinely as part of the HERMES experiment since its installation in May 1998. After the mirror alignment, the single photon resolution of the detector is within 10% of the Monte Carlo predictions. The particle identification based on the inverse ray tracing technique has been implemented and its likelihood analysis is being optimized. More elaborate particle identification schemes, especially those that are based on event level algorithms, are currently under development. Hadron identification by the RICH detector will be a crucial feature of the analysis of the current (1998 and 1999) and future HERMES data.

*TJNAF; †Jet Propulsion Lab

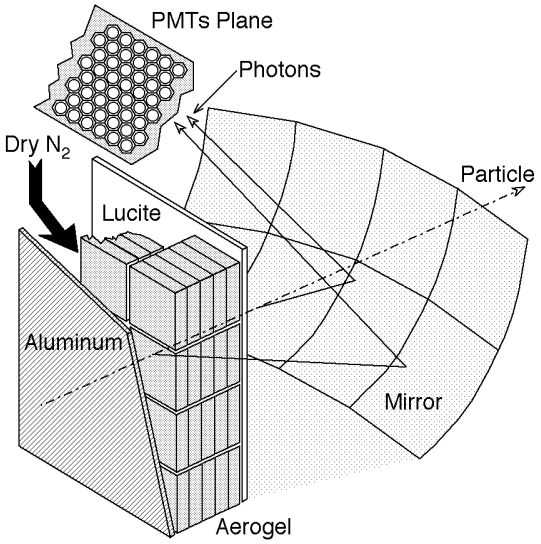

Fig. IV-8. Basic geometry and radiator configuration for the HERMES dual radiator RICH.

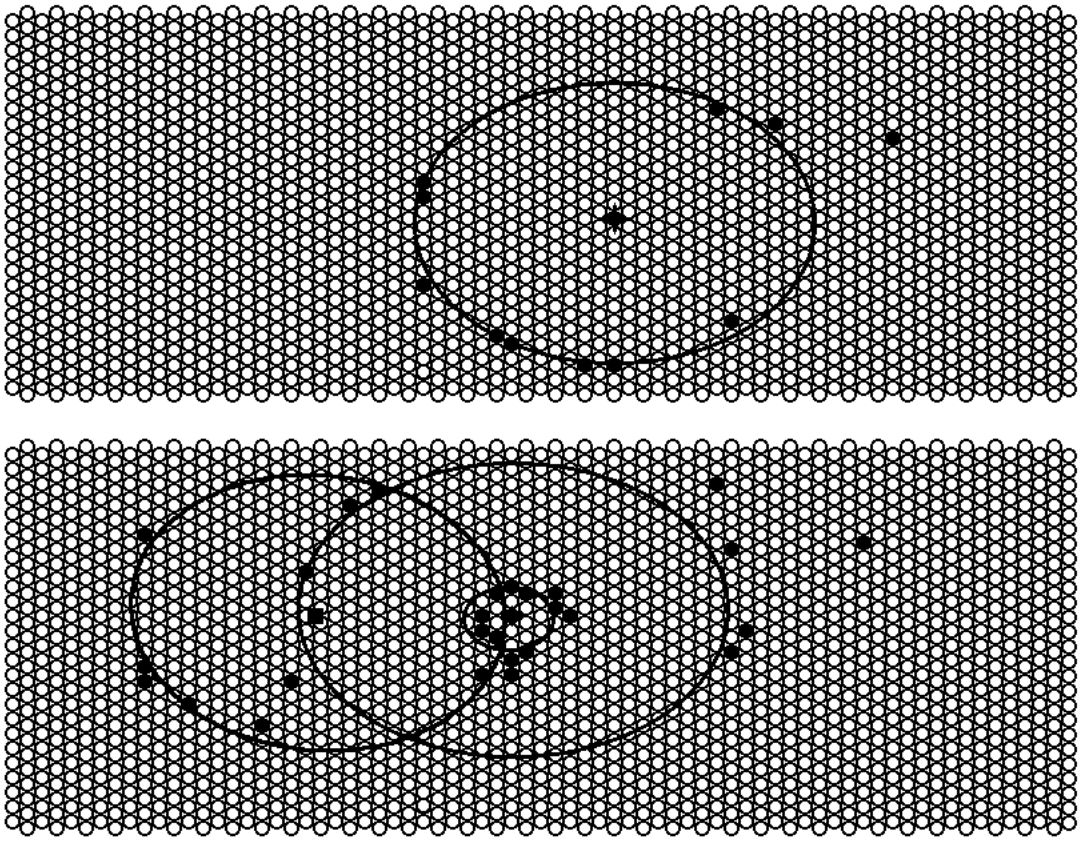

Fig. IV-9. HERMES RICH event display for an event with an electron and a pion in the lower half and a kaon in the upper half.

a.12. Lepton Pair Production with 800-Gev Protons to Explore the Antiquark Sea and ψ Production

(D. F. Geesaman, S. B. Kaufman, N. Makins, B. A. Mueller, P. E. Reimer, J. D. Bush,*L. D. Isenhower,* M. E. Sadler,* R. S. Towell,* J. L.Willis*, D. K.Wise*, C. N. Brown†, W. E. Cooper†, X. C. He‡,W. M. Lee‡, G. Peitt,‡ D. M. Kaplan,§ T. A. Cary;¶ G. T. Garvey,¶ D. M. Lee,¶ M. J. Leitch,¶ P. L. McGaughey,¶ T. N. Thompson,¶ P. N. Kirk,¶ Y. C. Wang,¶ Z. F. Wang,¶ M. E. Beddo,** T. H. Chang,** G. Kyle,** V. Papavassiliou,** J. Selden,** J. C. Webb,** T. C. Awes,†† P. W. Stankus,†† G. R. Young,†† E. A. Hawker,‡‡ G. A. Gagliardi,‡‡ R. E. Tribble,‡‡ M. A. Vasiliev,‡‡ D. D. Koetke,§§ and P. M. Nord§§)

While it is not required by any fundamental symmetry, it has—until recently—been widely assumed that distributions of anitdown ($\bar{d}$) and anti-up ($\bar{u}$) quarks in the proton sea were identical. After evidence from Deep Inelastic Scattering (DIS) of an integral difference between these distributions, the Fermilab 866/NuSea experiment measured the ratio of $\bar{d}/\bar{u}$ as a function of the momentum carried by the struck quark, x. Data were collected in 1996-1997 using the Meson East Spectrometer at Fermilab measuring Drell-Yan produced muon pairs from hydrogen and deuterium targets. Additional measurements of the nuclear dependence of J/ψ, ψ' and Drell-Yan production were made using Be, Fe and W targets.

The full analysis of the hydrogen and deuterium data is now complete. From the ratio of deuterium to hydrogen Drell-Yan cross sections, the ratio $\bar{d}/\bar{u}$ and the difference $\bar{d} - \bar{u}$ have been extracted. This revealed a striking, x -dependent asymmetry in the proton's antiquark sea. The flavor difference is a pure flavor non-singlet quantity: its integral is Q^2 independent and its Q^2 evolution, at leading order, does not depend on the gluon distributions in the proton. Therefore large differences seen in Fig. IV-10 must be nonperturbative in nature. Several approaches have been suggested to produce this difference[1], which include: (1) hadronic models of the meson cloud within the nucleon, (2) chiral quarks models which couple mesons directly to the constituent quarks, and (3) instanton models. These are illustrated by the curves in Fig. IV-10.

Although not well explained, the rate of production of the J/ψ and ψ' is diminished in nuclear targets relative to the same process with a proton target. Using nuclear targets, E866/NuSea is studying this suppression as a function of the kinematics variables Feynman- x (x_F) and transverse momentum. One significant observation, as shown in Fig. IV-11, is a difference between of the J/ψ and ψ' at low values of x_F, where the ψ' is suppressed more than the J/ψ. This affect might be attributable to the absorption of the $c\bar{c}$ pair in the nucleus before hadronization. Other effects, such as shadowing, also play important roles in the observed suppression.

Shadowing, which has been parameterized from DIS experiments, is also expected in Drell-Yan and J/ψ production data. By comparing the Drell-Yan yields from nuclear targets we were able to confirm that shadowing in Drell-Yan quantitatively matches predictions based on shadowing in DIS. In the Drell-Yan process, only initial state interactions are important since the final state muons do not interact with the nucleus. This, combined with the ability to correct for nuclear shadowing, makes Drell-Yan an ideal tool for the study of parton energy loss. Using the same data, corrected for shadowing, very tight limits were place on the energy loss of partons traveling through cold nuclear matter.

Analysis of the E866/NuSea Data continues, focusing on the following issues: (1) Extracting absolute Drell-Yan cross sections for hydrogen and deuterium. (2) Studying the angular distributions of ψ' production, which does not suffer from contamination by decays from higher $c\bar{c}$ states. (3) Extraction of Υ angular distributions. The latter two compliment the already analyzed data on the polarization of J/ψ production which will be compared with models formulated to reproduce higher energy collider data.

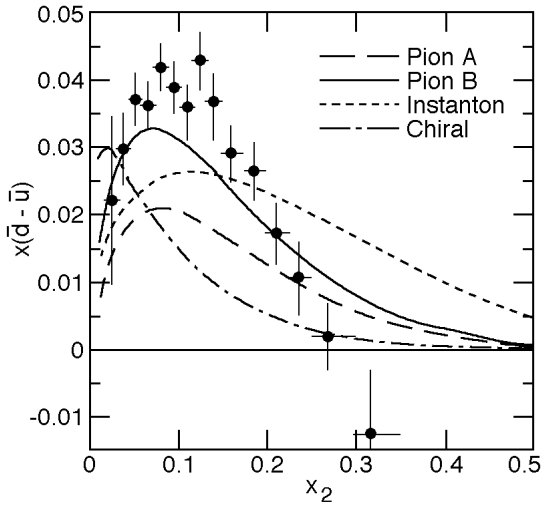

Fig. IV-10. The x dependence of the difference x ($\bar{d}$ − $\bar{u}$) of the proton at a mass scale of 7.353 GeV. The curves represent several model calculations[1]. The "pion cloud" curves show the effect of different vertex cutoffs.

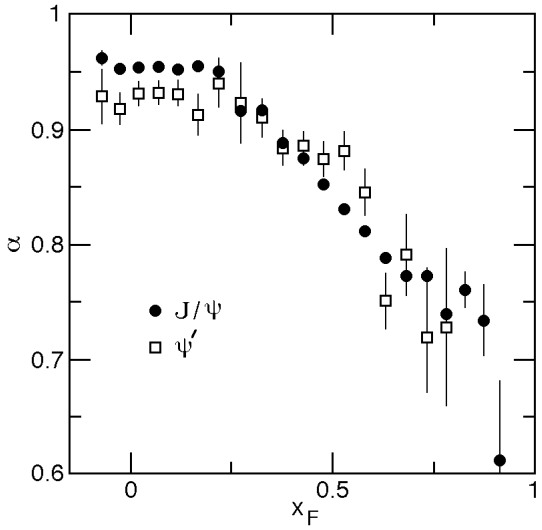

Fig. IV-11. Nuclear suppression of J/ψ and ψ' production parameterized in terms of a where $\sigma_A = \sigma_p A^{\alpha}$ and σ_A , σ_p represent the production cross section on a nuclear target and a free proton, respectively.

*Abilene Christian University; †Fermi National Accelerator Laboratory; ‡Georgia State University; §Illinois Institute of Technology; ¶Los Alamos National Laboratory; ||Louisiana State University; **New Mexico State University; ††Oak Ridge National Laboratory; ‡‡Texas A&M University; ¶Valparaiso University

[1]J. C. Peng *et al.*, Phys. Rev. D **58** 092004 (1998).

a.13. ϒ and J/ψ Production from 800-GeV Protons Incident on D_2 and H_2 Targets

(D. F. Geesaman, S. B. Kaufman, N. Makins, B. A. Mueller, J. D. Bush,* L. D. Isenhower,* M. E. Sadler,* R. S. Towell,* J. L. Willis,* D. K. Wise,* C. N. Brown,† W. E Cooper,† X. C. He,‡ W. M. Lee,‡ G. Petitt, ‡ D. M. Kaplan,§ T. A. Cary,¶ G. T. Garvey,¶ D. M. Lee,¶ M. J. Leitch,¶ P. L. McGaughey,¶ J. M. Moss,¶ B. K. Park,¶ J. C. Peng,¶ P. E. Reimer,¶ W. E. Sondheim,¶ T. N. Thompson,¶ P. N, Kirk,|| Y. C. Wang,|| Z. F. Wang,|| M. E. Beddo,** T. H. Chang,** G. Kyle,** V. Papavassiliou,** J. Selden,** J. C. Webb,** T. C. Awes,†† P. W. Stankus,†† G. R. Young,††, E. A. Hawker,‡‡ C. A. Gagliardi,‡‡ R. E. Tribble,‡‡ M. A. Vasiliev,‡‡ D. D. Koetke,§§ and P. M. Nord§§)

Fermilab experiment E866 is designed to detect pairs of oppositely charged muons produced in collisions between 800 GeV protons and variety of fixed targets. The primary motivation for E866 was to detect dimuon events generated in Drell-Yan reactions, but the detector is sensitive to any process which produces dimuon pairs. One such process is heavy quark vector meson production. ϒ and J/ψ particles are produced when partons from the beam and target annihilate and form a virtual gluon which then hadronizes into a heavy resonance state. These states have several percent branching ratios into dimuon pairs and are detected during normal data acquisition. The virtual gluon which produce the resonance can be generated by the annihilation of either a quark/antiquark pair or a pair of gluons. Resonance production is therefore sensitive to both the quark and gluon distributions within the beam and target. J/ψ production is believed to occur dominantly via gluon-gluon fusion, while ϒ production is thought to have contributions from both gluon-gluon fusion and quark-antiquark annihilation. Because the gluon distribution for the proton and neutron are thought be the same, the per nucleon J/ψ production cross section is expected to be the same for hydrogen and deuterium. The ϒ production ratio, on the other

hand, is expected to be larger than unity since $\bar{u}_n(x) > \bar{u}_p(x)$ for the Bjorken-x values of ϒ production accessed in E866.

The E866 hydrogen and deuterium data samples contain approximately 30000 ϒ and 1 million J/ψ events. The production cross sections are determined by fitting the measured mass distribution to the simulated mass distributions of the relevant vector mesons and the underlying Drell-Yan continuum. This separation is performed for several bins in X-Feynman, to determine the kinematic dependence of the cross section. The absolute ϒ and J/ψ production cross sections for hydrogen and deuterium are obtained from the extracted results by normalizing the yields to the integrated luminosity and correcting the results by the acceptance of the detector. The cross sections values can then be compared to predictions based various models using the various parton distributions available in the literature. Color evaporation model (CEM) calculations have been performed for both J/ψ and ϒ production from H_2 and D_2. Although the CEM model is extremely simple and cannot predict the absolute value of the cross sections, the X-Feynman shape is reproduced by the CEM calculation. Further, the unknown scale factor in the CEM calculations cancels when the D_2/H_2 per-nucleon ratio is calculated. The extracted cross section ratio, D/2H , for J/ψ and ϒ production are shown in Fig. IV-12. The J/ψ ratio is close to unity, which is consistent with expectations assuming gluon fusion production. The ϒ ratio is also consistent with unity, which is in disagreement with the CEM calculation when either the MRST or CTEQ5M parton distribution functions (PDFs) are used. The deviation from the prediction may indicate that the PDFs underestimate the hard gluon (x ≈ 0.25) distribution in the proton.

*Abilene Christian University; †Fermi Na;tional Accelrator Laboratory; ‡Georgia State University; §Illinois Institute of Technology; ¶Los Alamos National Laboratory; || Louisiana State University; **New Mexico State University; ††Oak Ridge National Laboratory; ‡‡Texas A&M University; §§Valparaiso University

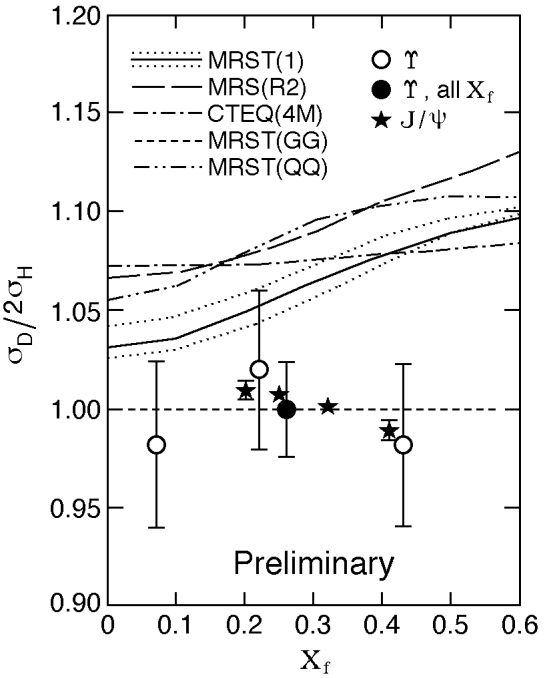

Fig. IV-12. The data points show the ratio of cross sections for υ and J/ψ production from deuterium and hydrogen. The curves correspond to color evaporation model calculations using several different parameterizations for the nucleon parton distributions.

a.14. Lepton Pair Production with 120-GeV Protons to Extend the Measurement of $\bar{d}/\bar{u}$ in the Nucleon

(D. DeSchepper, D. F. Geesaman, B. A. Mueller, T. G. O'Neill, D. H. Potterveld, P. E. Reimer, L. D. Isenhower*, M. E. Sadler*, C. N. Brown,† G. T. Garvey,‡ M. J. Leitch,‡ P. L. McGaughey,‡ J.-C. Peng,‡ R. Gilman,§ C. Glashausser,§ X. Jiang,§ R. Ransome,§ S. Strauch,§ C. A. Gagliardi,¶ R. E. Tribble,¶ M. A. Vasiliev,¶ and D. D. Koetke||)

The measurement by the Fermilab 866/NuSea Experiment revealed an unexpected dependence of the $\bar{d}/\bar{u}$ ratio on the momentum fraction of the struck quark, x. For $x > 0.19$ the antiquark asymmetry began to decline, returning to a completely symmetric sea near the highest values of x accessible to the experiment. A significant extension of the x -range can be achieved with a higher-intensity, lower-energy beam, making this a study ideally suited for a "slow extraction" beam from the 120 GeV Fermilab main injector. The expected statistical errors which could be obtained from such a measurement are shown in Fig. IV-13.

After a favorably received letter of intent, a full proposal for this measurement was submitted to Fermilab in the spring of 1999. At that time, the Fermilab decided not to commit to a fixed target program based on a slow extraction because of its effect on the collider luminosity and the time scales of the other experiments which were proposed for this type of beam. The collaboration was encouraged to submit a proposal in the spring of 2001 when the impact of a fixed target program will be reconsidered. The collaboration intends to resubmit a new proposal at this time, and work is continuing toward this end.

*Abilene Christian University; †Fermi National Accelerator Laboratory; ‡Los Alamos National Laboratory; §Rutgers University; ¶Texas A&M University; ||Valparaiso University

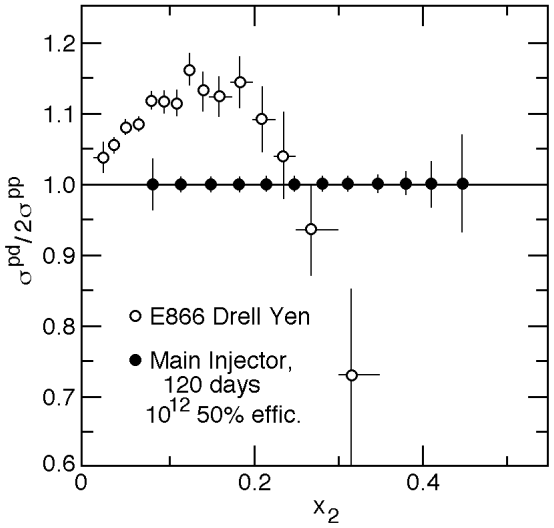

Fig. IV-13. Expected statistical precision for the proposed experiment (error bars with solid circles) arbitrarily plotted at a ratio of 1.0. Systematic errors are estimated to be less than 1%. Also shown are the Fermilab E866/NuSea results (open circles) for the x -dependence of the ratio of Drell-Yan cross sections from deuterium and hydrogen.

B. ATOM TRAP TRACE ANALYSIS

b.1. A New Method of Ultrasensitive Trace-Isotope Analysis

(K. Bailey, C. Y. Chen, X. Du, Y. M. Li, Z.-T. Lu, T. P. O'Connor, and L. Young*)

We have demonstrated a new method of ultrasensitive trace-isotope analysis[1]. Named Atom Trap Trace Analysis (ATTA), this method is based on the techniques of laser cooling and trapping of neutral atoms, and has been used to count individual ^{85}Kr($t_{1/2}$ = 10.8 yr) and ^{81}Kr($t_{1/2} = 2 \times 10^5$ yr) atoms present in a natural krypton gas sample with isotopic abundances in the range of 10^{-11} and 10^{-13}, respectively.

In 1999, we characterized and optimized the atomic beam machine that was built in 1998. With this machine, the abundant ^{83}Kr (11.5%) atoms could be loaded into the trap at 3×10^8 sec^{-1}, or about 2×10^{-7} of the ^{83}Kr atoms injected into the vacuum system. The total efficiency resulted from a combination of the efficiency of metastable atom production (~10^{-4}), losses due to atomic beam divergence (~10^{-3}), and the fraction of atoms captured while passing through the trap (~10^{-1}). In order to optimize both capture efficiency and the sensitivity of single atom detection, we implemented a procedure that alternated trap parameters between two sets that were optimized for capture and detection respectively. We could clearly detect a single trapped atom by observing its fluorescence, with a signal equal to 50 times the background noise (Fig. IV-14). We have detected and counted ^{81}Kr and ^{85}Kr atoms in an atmospheric krypton sample (Fig. IV-15), and measured the isotopic abundances to be $(1.5 \pm 0.4) \times 10^{-11}$ for ^{85}Kr and $(1.0 \pm 0.4) \times 10^{-12}$ for ^{81}Kr.

For real-world applications such as radio-krypton dating of ancient groundwater or polar ice, a much higher efficiency (10^{-4}-10^{-3}) is required. In order to improve the efficiency, we are currently investigating different methods of producing metastable krypton atoms. In addition, we plan to cool the atom source and recirculate the krypton atoms in the vacuum system.

In the future, ATTA can be used to analyze many other isotope tracers for a wide range of potential applications including measuring solar neutrino flux, searching for exotic particles, tracing atmospheric and oceanic currents, archeological and geological dating, medical diagnostics, and monitoring fission products in the environment for safe-guarding nuclear wastes.

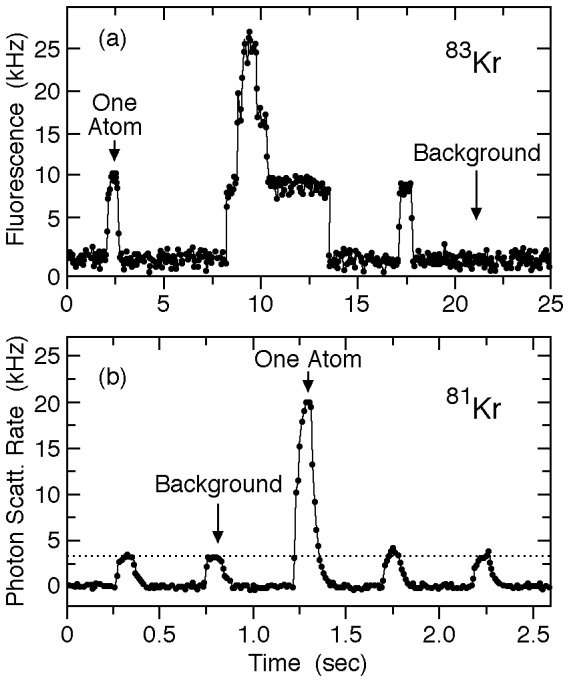

Fig. IV-14. Single atom counting. (a) Changes of the fluorescence signal of the abundant ^{83}Kr atoms mark the arrival and departure of individual atoms in the laser trap. (b) Signal of a single trapped ^{81}Kr atom. During loading time, the photon-count rate was low because the counter was blocked for protection from over-exposure.

*Chemistry Division, ANL

[1]C. Y. Chen et. al., Science **286**, 1139 (1999).

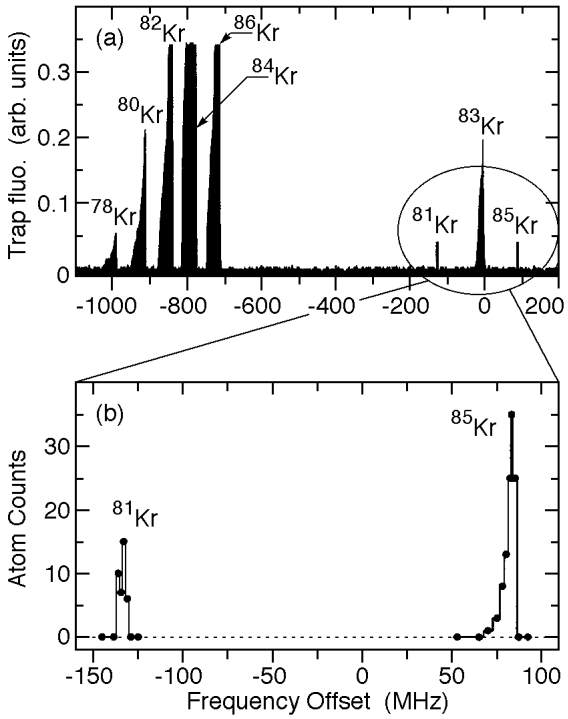

Fig. IV-15. The fluorescence signal from laser trapped metastable krypton atoms. Atoms of different isotopes are trapped at different laser frequencies due to isotope shifts. (a) The signal of abundant Kr isotopes; (b) Number of ^{81}Kr and ^{85}Kr atoms counted vs. laser frequency. Each data point represents the number of atoms counted in 3 hours for ^{81}Kr and 0.5 hours for ^{85}Kr.

b.2. Atom Trap Trace Analysis of ^{41}Ca

(K. Bailey, X. Du, Y. M. Li, Z.-T. Lu, T. P. O'Connor, and L. Young*)

Calcium is an essential element in biological and geological objects. In particular, its abundance in human bones has motivated many works on the trace analysis of ^{41}Ca ($t_{1/2}$=103 kyr) for important applications in medicine and archaeology. In medicine, ^{41}Ca-tracer can be used to monitor bone-loss rates thereby providing an effective tool in the diagnosis of osteoporosis as well as in the evaluation of its treatment. In archaeology, ^{41}Ca is a potential tracer for dating bones in the age range of 10^5 years. This is an important era in human development, but is too old to be dated with ^{14}C ($t_{1/2}$=5.7 kyr)

So far, accelerator mass spectrometry (AMS) has been the only method available for these applications[1]. The natural isotopic abundance of ^{41}Ca(~10^{-15}) has been measured using AMS. A complete systematic study, however, has not been possible because the AMS detection limit is too close to the natural level. For medical applications, where the isotopic abundance of ^{41}Ca can be artificially raised to as high as 10^{-10}, AMS has proven to be an effective method in research works, however, its cost is likely to prevent it from being accessible to the general medical community.

We are developing a ^{41}Ca analyzer using the new Atom Trap Trace Analysis(ATTA) method[2], with the goal of advancing both of the aforementioned applications. ATTA is immune to contamination from other elements and isotopes, and has the potential to reach a detection limit far below the natural isotopic abundance of ^{41}Ca. Compared with a typical AMS facility, an ATTA apparatus is significantly cheaper and occupy a smaller area. Therefore, ATTA has a much better

chance of becoming a generally accessible medical instrument.

In 1999, we have installed a laser system that generates the 423nm laser light needed to trap calcium atoms. We have designed a calcium atomic beam machine and ordered various parts. Assembly and characterization of this system will be carried out in the following year.

*Chemistry Division, ANL

[1]W. Henning et. al., Science **236**, 725 (1987). D. Elmore et. al., Nucl. Instr. Meth. **B52**, 531 (1990).
[2]C. Y. Chen et. al., Science **286**, 1139 (1999).

b.3. Laser Spectroscopy of Rare Isotopes

(K. Bailey, C. Y. Chen, X. Du, Y. M. Li, Z.-T. Lu, T. P. O'Connor, and L. Young*)

Laser spectroscopy on atoms has long been used to determine nuclear properties such as spins, magnetic dipole moments, electric quadrupole moments, and charge radii. In order to study unstable and rare isotopes, we have developed a sensitive atom trap trace analysis technique[1] to trap and conduct laser spectroscopy on individual atoms. When coupled with an ISOL source, this technique can be used to study, for example, short-lived cesium isotopes or neutron-rich ^{6}He and ^{8}He isotopes.

In 1999, we have conducted laser spectroscopy on individual ^{85}Kr atoms in the trap, and demonstrated the sensitivity of this technique. From a total of ~10^{9} ^{85}Kr atoms injected into the atom source, we trapped 145 atoms and obtained the spectrum shown in Fig. IV-16. The data points were on one side of the peak because trapping is only possible with the laser frequency tuned below the atomic resonance. A full and more precise spectrum can be obtained with improvements such as separating the processes of trapping and fluorescence collection.

*Chemistry Division, ANL

[1]K. Bailey et. al., A new method of ultrasensitive trace-isotope analysis, Physics Division Annual Report, ANL-99.
[2]B. D. Cannon, Phys. Rev. **A47**, 1148 (1993).

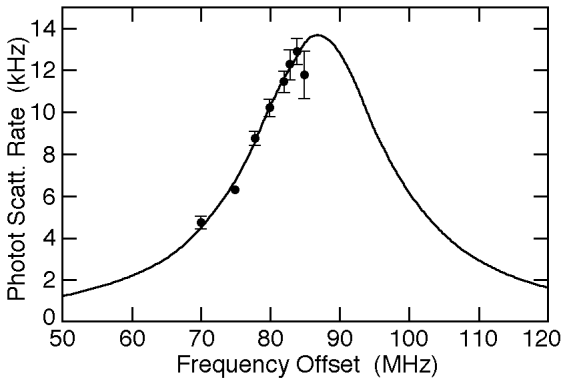

Fig. IV-16. Single atom fluorescence versus laser frequency offset. The measured photon-count rates are fitted to a Lorentzian function, rates $[(f-f_r)^2 + (\gamma/2)^2\Gamma]^{-1}$. *Here,* f_r *is the resonant transition frequency of* ^{85}*Kr, f is the laser frequency, and* $\gamma = \Gamma(1+s)^{1/2}$ *is the power-broadened linewidth. We fixed* f_r *= 87 MHz and* Γ *= 5.3 MHz according to previous spectroscopy measurements*[2]. *The resulting saturation parameter s = 19* ± *1. Error bars represent the change in fluorescence between different atoms. We attribute the cause of large fluctuations near resonance to the fact that the atom trajectory partially extends beyond the viewing region as the trap temperature increases near resonance.*